ACCOUNTS of chemical research

pubs.acs.org/accounts Article

Molecular and Supramolecular Designs of Organic/Polymeric Micro-photoemitters for Advanced Optical and Laser Applications

Yohei Yamamoto,* Hiroshi Yamagishi, Jer-Shing Huang, and Axel Lorke

Cite This: *Acc. Chem. Res.* 2023, 56, 1469−1481 Read Online

ACCESS | Metrics & More | Article Recommendations

CONSPECTUS: For optical and electronic applications of supramolecular assemblies, control of the hierarchical structure from nano- to micro- and millimeter scale is crucial. Supramolecular chemistry controls intermolecular interactions to build up molecular components with sizes ranging from several to several hundreds of nanometers using bottom-up self-assembly process. However, extending the supramolecular approach up to a scale of several tens of micrometers to construct objects with precisely controlled size, morphology, and orientation is challenging. Especially for microphotonics applications such as optical resonators and lasers, integrated optical devices, and sensors, a precise design of a micrometer-scale object is required. In this Account, we review the recent progress on precise control of microstructures from π-conjugated organic molecules and polymers, which work as micro-photoemitters and are suitable for optical applications.

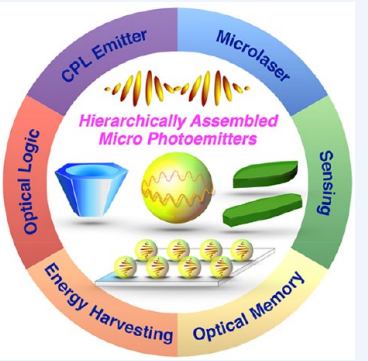

After the introduction on the importance of the control of the hierarchical structures from molecular assembly, we review supramolecular methodology for assembling molecules and supramolecules to form microstructures such as spheres and polygons with precisely controlled morphology and molecular orientations. The resultant microstructures act as anisotropic emitters of circularly polarized luminescence. We report that synchronous crystallization of π-conjugated chiral cyclophanes forms concave hexagonal pyramidal microcrystals with homogeneous size, morphology, and orientation, which clearly paves the way for the precise control of skeletal crystallization under kinetic control. Furthermore, we show microcavity functions of the self-assembled micro-objects. The self-assembled π-conjugated polymer microspheres work as whispering gallery mode (WGM) optical resonators, where the photoluminescence exhibits sharp and periodic emission lines. The spherical resonators with molecular functions act as long-distance photon energy transporters, convertors, and full-color microlasers. Fabrication of microarrays with photoswitchable WGM microresonators by the surface self-assembly technique realizes optical memory with physically unclonable functions of WGM fingerprints. All-optical logic operations are demonstrated by arranging the WGM microresonators on synthetic and natural optical fibers, where the photoswitchable WGM microresonators act as a gate for light propagation via a cavity-mediated energy transfer cascade. Meanwhile, the sharp WGM emission line is appropriate for utilization as optical sensors for monitoring the mode shift and mode splitting. The resonant peaks sensitively respond to humidity change, absorption of volatile organic compounds, microairflow, and polymer decomposition by utilizing structurally flexible polymers, microporous polymers, nonvolatile liquid droplets, and natural biopolymers as media of the resonators. We further construct microcrystals from π-conjugated molecules with rods and rhombic plates, which act as WGM laser resonators with light-harvesting function. Our developments, precise design and control of organic/polymeric microstructures, form a bridge between nanometer-scale supramolecular chemistry and bulk materials and pave the way toward flexible micro-optics applications.

KEY REFERENCES

- Oki, O.; Kulkarni, C.; Yamagishi, H.; Meskers, S. C. J.; Lin, Z.-H.; Huang, J.-S.; Meijer, E. W.; Yamamoto, Y. Robust Angular Anisotropy of Circularly Polarized Luminescence from a Single Twisted-bipolar Polymeric Microsphere. *J. Am. Chem. Soc.* **2021**, *143*, 8772−8779.[1] *Chiral conjugated polymers self-assemble to form micro-spheres with twisted bipolar configuration that exhibit angularly anisotropic circularly polarized luminescence, evidenced by angular-dependent single-particle measure-ments.*
- Oki, O.; Yamagishi, H.; Morisaki, Y.; Inoue, R.; Ogawa, K.; Miki, N.; Norikane, Y.; Sato, H.; Yamamoto, Y. Synchronous assembly of chiral skeletal single-crystalline microvessels. *Science* **2022**, *377*, 673−678.[2] *Vessel-like*

Received: February 13, 2023
Published: May 23, 2023

https://doi.org/10.1021/acs.accounts.3c00084
Acc. Chem. Res. 2023, 56, 1469−1481

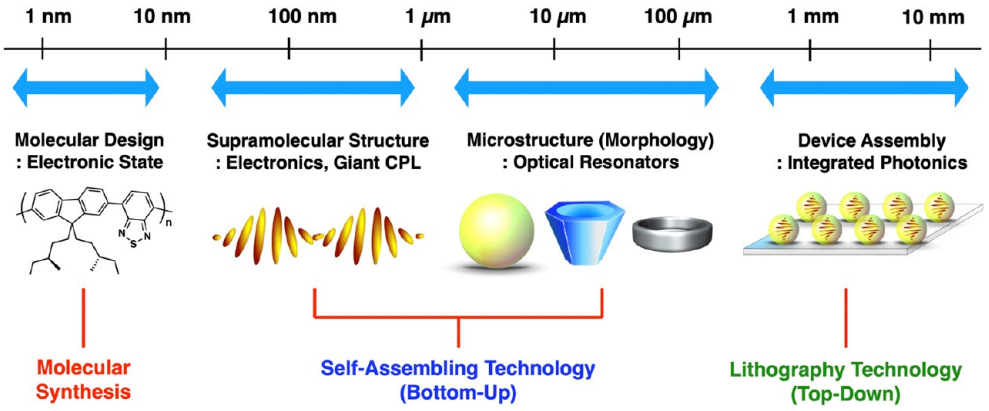

Figure 1. Schematic representation of the hierarchical structures of supramolecular materials at various length scales and the corresponding properties for device applications.

skeletal microcrystals are grown synchronously with homogeneous size, shape, and orientation from planar-chiral cyclophane molecules.

- Tabata, K.; Braam, D.; Kushida, S.; Tong, L.; Kuwabara, J.; Kanbara, T.; Beckel, A.; Lorke, A.; Yamamoto, Y. Self-Assembled Conjugated Polymer Spheres as Fluorescent Microresonators. *Sci. Rep.* **2014**, *4*, 5902.[3] *Self-assembled π-conjugated polymer microspheres act as optical resonators, in which the confinement of the fluorescence light inside the sphere leads to whispering gallery modes with sharp and periodic emission lines.*
- Okada, D.; Lin, Z.-H.; Huang, J.-S.; Oki, O.; Morimoto, M.; Liu, X.; Minari, T.; Ishii, S.; Nagao, T.; Irie, M.; Yamamoto, Y. Optical microresonator arrays of fluorescence-switchable diarylethenes with unreplicable spectral fingerprints. *Mater. Horiz.* **2020**, *7*, 1801−1808.[4] *Photoswitchable optical resonator arrays consisting of the oxidized form of diarylethene can act as ultimate anti-counterfeiting optical memory devices with individually different whispering gallery mode fingerprints that act as physically uncloneable functions.*

1. INTRODUCTION

Organic light-emitting diodes (OLEDs) are commercially available nowadays as displays and lighting devices. Their advantages are light weight, flexibility, low power consumption, and high brightness and saturation. One of the important targets for the next area of research on organic electronics and photonics is the realization and application of organic lasers.[5] It is of practical importance to realize electrically driven organic lasers,[6] but also for the fundamental research aspects, it is of great interest to realize lasers from organic and polymeric materials, such as microlasers, flexible lasers, polaritonic lasers, and lasers for sensing applications. Especially, microresonators and microlasers are important for applications in optical integrated circuits, optical logic gates, optical barcodes, optical sensors, and imaging.[7]

For the realization of micrometer-scale optical resonators and lasers from organic molecules and polymers, precise control of the microstructure is important. Representative micrometer-scale resonators are Fabry−Pérot (FP) resonators and whispering gallery mode (WGM) resonators.[8,9] A FP resonator typically consists of well-faceted microcrystals, where the two facets work as parallel reflective surfaces and light is confined between these two mirrors. On the other hand, WGM resonators have ring, disk, sphere, or polygonal morphologies, and the light is confined circularly at the circumference of the microstructures via total internal reflection (TIR) at the interface between the high-index material and low-index surroundings. In general, two approaches are known to fabricate microstructures: The top-down approach by photolithography or electron-beam lithography and the bottom-up approach by molecular self-assembly. Especially, the self-assembly approach has benefits of being a simple yet massively parallel fabrication process with low cost and low energy consumption. It has therefore attracted increasing attention from chemists and materials scientists.

For applications of supramolecular assemblies in optical and electronic materials, systems, and devices, control of the hierarchical structure is crucial (Figure 1).[10,11] Design of the molecular structure is in the smallest scale (∼nanometer), which directly affects the electronic properties of the materials. The next level on a scale of several tens to several hundreds of nanometers is the supramolecular structure dominated by intermolecular interactions. Further control of the self-assembling morphologies at several to several tens of micrometers scale is required for optical resonators with efficient light confinement inside the microstructure. The micrometer-scale structure is appropriate for confining sub-micrometer-wavelength light with small mode volume. Finally, integration of the microstructures with appropriate orientation and arrangement is important for practical device applications for integrated photonics, memories, and displays.

In this Account, we review our recent progress on the precise control of self-assembled π-conjugated organic/polymeric light-emitting microstructures for optical and laser applications. Microstructures consisting of π-conjugated materials have various merits: [1] The microstructures work as both optical resonator and fluorophore, therefore no doping with fluorescent dyes is needed. [2] π-Conjugated molecules have high photoabsorptivity and a high refractive index in comparison with nonconjugated molecules, which is beneficial for efficient light absorption at the surface and confinement of light. [3] A simple fabrication process by bottom-up self-assembly is available. [4] Molecular functionality can be combined with the resonators. [5] π-Conjugated molecules have charge injection and charge transport properties, opening up the possibility of direct electrical excitation. By taking advantage of these characteristics, we construct optical microresonators and lasers with novel photonic functions, some of which are utilized

https://doi.org/10.1021/acs.accounts.3c00084
Acc. Chem. Res. 2023, 56, 1469−1481

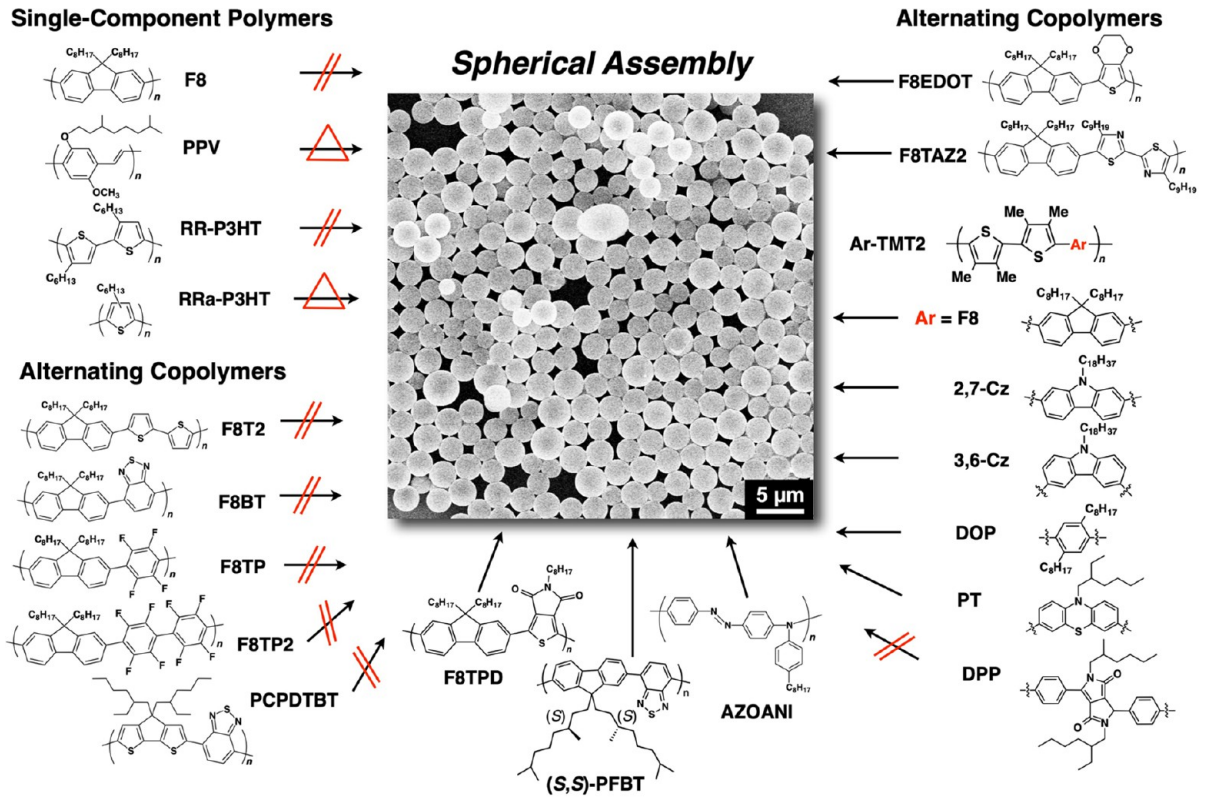

Figure 2. Molecular structures of π-conjugated polymers and self-assembled microspheres by a vapor diffusion method. The red-double lines indicate that the polymers hardly form microspheres. The red triangles indicate that the polymers form microspheres, but the surface morphology is rough.

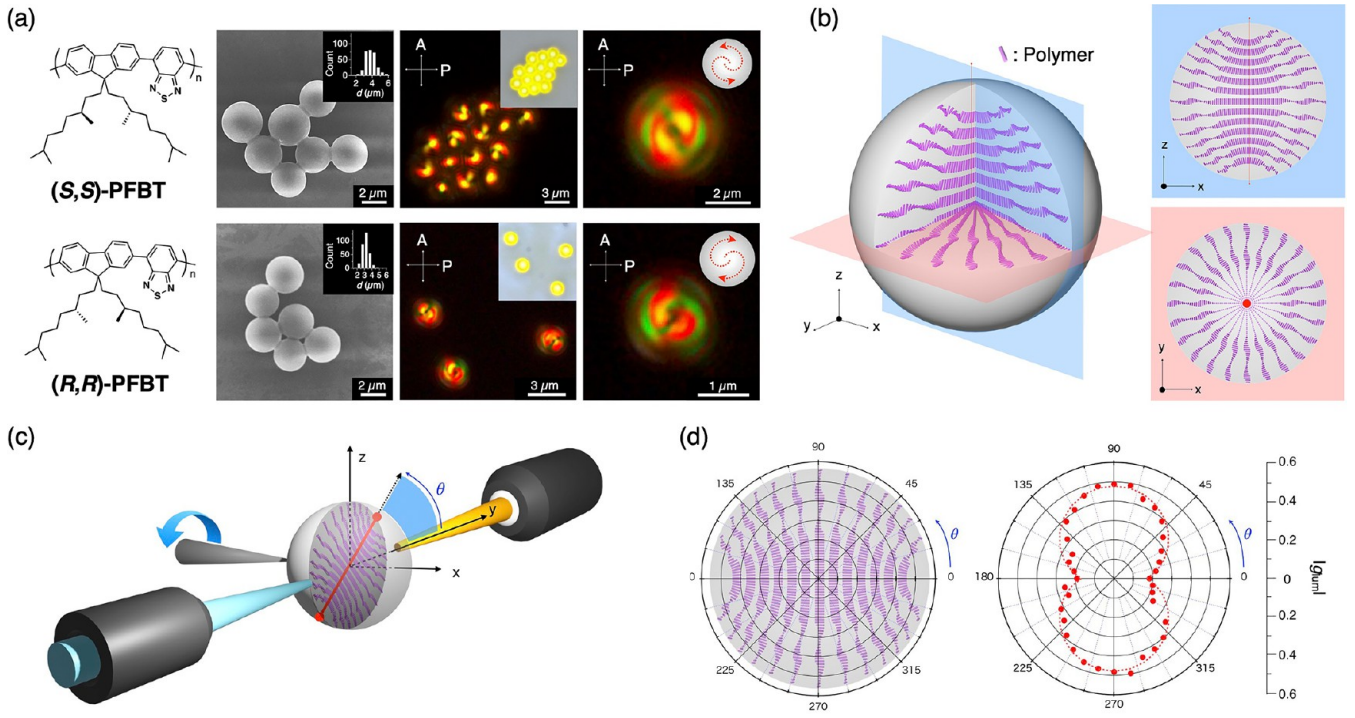

Figure 3. (a) Molecular structures of (*S*,*S*)- and (*R*,*R*)-PFBT and the self-assembled microspheres observed by SEM, POM, and OM. (b) Schematic representations of the TB configuration of the polymers in the microsphere. (c) Schematic representation of the experimental setup for angular anisotropy of CPL from a single particle. (d) Polar plot of *g*-value versus θ. Reproduced from ref 1. Copyright 2021 American Chemical Society.

for highly sensitive sensors, angularly anisotropic circularly polarized luminescence (CPL) emitters, and micrometer-scale vessels. Our achievements are an important step forward to the future molecular microphotonics applications.

https://doi.org/10.1021/acs.accounts.3c00084
Acc. Chem. Res. 2023, 56, 1469−1481

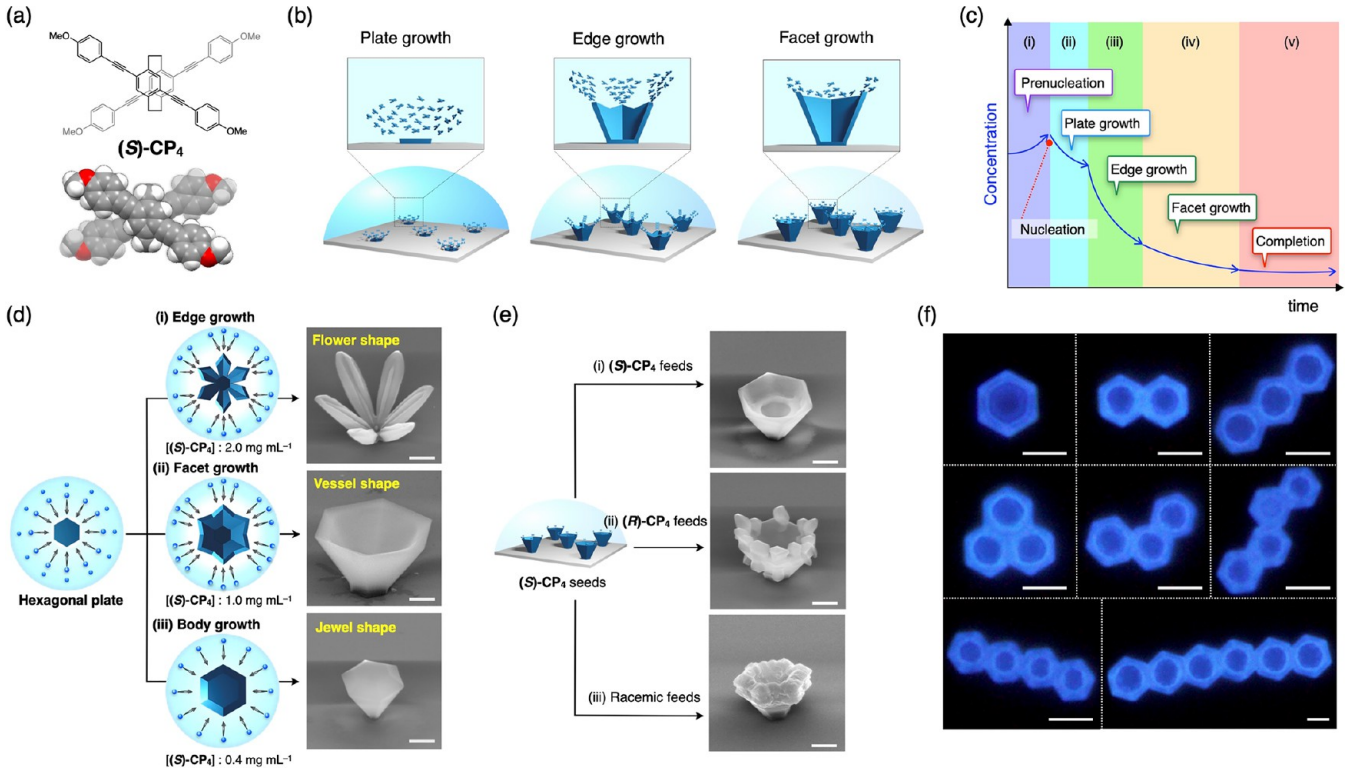

Figure 4. (a) Molecular structure of (*S*)-CP_4. (b) Schematic representations of the synchronous and uniaxial skeletal crystal growth regimes with plate, edge, and facet growth. (c) Schematic diagram depicting how concentration of (*S*)-CP_4 changes over time. (d) Schematic representation of (i) edge-, (ii) facet-, and (iii) body-growth crystallizations with respect to the different initial concentrations of (*S*)-CP_4 and corresponding SEM micrographs. (e) Scheme of the stepwise crystal growth and hierarchical microstructures after adding EtOH solutions of (i) (*S*)-CP_4, (ii) (*R*)-CP_4, and (iii) their racemic mixture to the vessel-shaped crystal seeds of (*S*)-CP_4 and corresponding SEM micrographs. (f) Fluorescent microscope (FM) images of fused microvessel crystals. Scale bars: 3 μm. Reproduced from ref 2. Copyright 2022 AAAS.

2. SUPRAMOLECULAR METHODOLOGY FOR ASSEMBLING MICRO-PHOTOEMITTERS

Most optical devices have been made from materials that feature tunable optical transmittance, reflectance, scattering, refraction, etc. Not only the intrinsic optical properties but also their morphology are finely adjusted so that the resultant materials display the desired properties. Photolithography has been the most reliable method to meet these requirements. However, photolithography is hardly applicable to most of the functional organic materials because their functions are readily damaged by photoexposure, development, and lift-off processes. We envisioned that molecular self-assembly could be a powerful method to turn the functional organic materials into optically functional morphologies.

2.1. Self-Assembled Microspheres from π-Conjugated Polymers

π-Conjugated polymers potentially have a variety of optical and electronic properties such as photoabsorption, luminescence, high refractive index, redox activity, and charge and energy transportation, which make these materials one of the major players in organic electronics and photonics.[12] For applications of π-conjugated polymers as semiconductors, high charge carrier mobility is one of the most important factors; therefore, a flat π-conjugated plane and rigid interpolymer aggregation are indispensable. Meanwhile, for luminescent applications, such strong interpolymer $\pi-\pi$ stacking and the resultant highly crystalline domains causes exciton annihilation, red shift, and suppression of the luminescence efficiency from the local exciton state.[13] To avoid these drawbacks, introduction of bulky side chains to twist the π-conjugated planes is an effective strategy for the formation of amorphous aggregates. We found that introduction of four methyl groups to the thiophene moieties in poly[(9,9-dioctylfluorenyl-2,7-diyl)-*alt*-(bithiophene-2,5-diyl)] induces a highly twisted main chain with dihedral angles between the adjacent aromatic rings of 44−67°, which suppresses $\pi-\pi$ stacking and leads to the formation of amorphous, well-defined microspheres.[14,15] To validate the generality of this strategy, self-assembly of more than 30 conjugated polymers was attempted.[16−27] The results show that π-conjugated polymers with high rigidity, planarity, and linearity hardly form spherical aggregates, while those with flexible or largely twisted main chains tend to form amorphous microspheres (Figure 2). By spectroscopic monitoring of the self-assembly behavior of highly linear poly[(9,9-dioctylfluorenyl-2,7-diyl)-*alt*-(5-octylthieno-[3,4-*c*]pyrrole-4,6-dione)] (F8TPD), a stepwise self-assembly was observed, the first step being the intrapolymer helical folding and the second step being the interpolymer aggregation to form microspheres.[18]

While most microspheres form amorphous aggregates, chiral conjugated polymers (*S*,*S*)- and (*R*,*R*)-poly(fluorene-*alt*-benzothiadiazole) (PFBT) form microspheres with definite birefringence as observed by polarized optical microscopy (POM), indicating that the obtained microspheres exhibit internal molecular order (Figure 3a).[1,28] From careful analysis of POM and transmission electron microscopy (TEM) of the sliced microsphere specimens, it was concluded that these microspheres possess twisted-bipolar (TB) configurations with helical cholesteric order of the polymer main chains (Figure 3b). The

https://doi.org/10.1021/acs.accounts.3c00084
Acc. Chem. Res. 2023, 56, 1469−1481

optical microscope (OM) monitoring of the assembly process clearly indicates that the formation of the microspheres involves liquid−liquid phase separation and subsequent lyotropic liquid crystalline mesophase formation. Due to the TB configuration with topological defects at the bipolar axis, the morphologically isotropic microspheres display remarkable angular anisotropy of CPL, evidenced by single-particle CPL experiments (Figure 3c,d). This is the first experimentally observed angular anisotropy of CPL from a supramolecular assembly.

2.2. Self-Assembly of Micrometer-Scale Crystalline Particles

In the studies on the crystallization of π-conjugated molecules on a substrate surface, we discovered synchronous assembly of planar-chiral π-conjugated cyclophane to form skeletal microcrystals with homogeneous size, shape, and orientation on a whole surface.[2] In general, under thermodynamic conditions in solution, crystallization occurs in thermal equilibrium, resulting in the formation of crystals with convex polyhedral morphology. Meanwhile, under diffusion-limited conditions, crystals grow kinetically, resulting in the formation of skeletal crystals with concave morphology such as two-dimensional dendrite crystals and three-dimensional hopper crystals. However, under the kinetic conditions, the crystallization process is difficult to control. Therefore, in the crystal engineering research field, the precise control of size, shape, and orientation of skeletal crystals is a big challenge.

A powder of planar-chiral π-conjugated cyclophane, (*S*)-CP_4 or (*R*)-CP_4, was dispersed in EtOH and heated to its boiling point (~70 °C) (Figure 4a).[29] Then, the solution was drop cast on a quartz substrate, and vessel-shaped hexagonal pyramidal microcrystals were grown vertically on the substrate within 10 s. The average diameter of the hexagonal inscribed circle is 4.3 μm, and the crystal size is monodisperse with a polydispersity index of 0.41×10^{-2}. As determined by careful observation of the crystal growth process, the hexagonal plate-like crystal nucleation takes place at the substrate surface within a short time period of 2.0−2.1 s after the drop casting of the solution, and subsequently, the hexagonal pyramidal crystals grow within 10 s via edge and facet growth (Figure 4b,c). By changing the initial concentration, the morphology of the resultant crystals is precisely controlled with flower-like dendritic crystals and jewel-like convex crystals (Figure 4d). The crystalline edge of the microvessel crystals recognizes the plane chirality, as evidenced by the stepwise feeds of the solution (Figure 4e). Furthermore, the vessel crystals behave as microscopic containers, keeping a tiny volume of liquid, and fuse with one another to form polycyclic aromatic hydrocarbon-like superstructures (Figure 4f).

3. FUNCTIONS OF MICRO-PHOTOEMITTERS MADE BY SELF-ASSEMBLY

Micro-photoemitters, when appropriately shaped by self-assembly, exhibit unique optical properties that are distinct from those of their bulk solid and solution states. This is mostly because of their unique molecular-scale order and three-dimensional morphology. Self-assembly usually allows the constituent molecules to stack with one another in a certain periodic manner. The periodicity ranges from several angstroms to micrometers, which is well beyond the typical size-tunability of photolithography. This sophisticated order enables novel optical functions such as angular anisotropy and circular asymmetry. Another characteristic of the self-assembled emitters is their three-dimensionally complicated morphology. Representative morphologies of the self-assembled particles include convex and concave polygons, spheres, ellipsoids, and tori. Such three-dimensional shaping is beyond the capabilities of conventional photolithography, which is predominantly geared toward two-dimensional manufacturing.

3.1. Fluorescent Microresonators from π-Conjugated Polymer Microspheres

Self-assembled π-conjugated polymer microspheres act as fluorescent microresonators. Upon focused laser irradiation to a single microsphere, the photoluminescence (PL) of a single microsphere exhibits sharp and periodic emission lines, superimposed upon the broad PL band (Figure 5a).[3] These

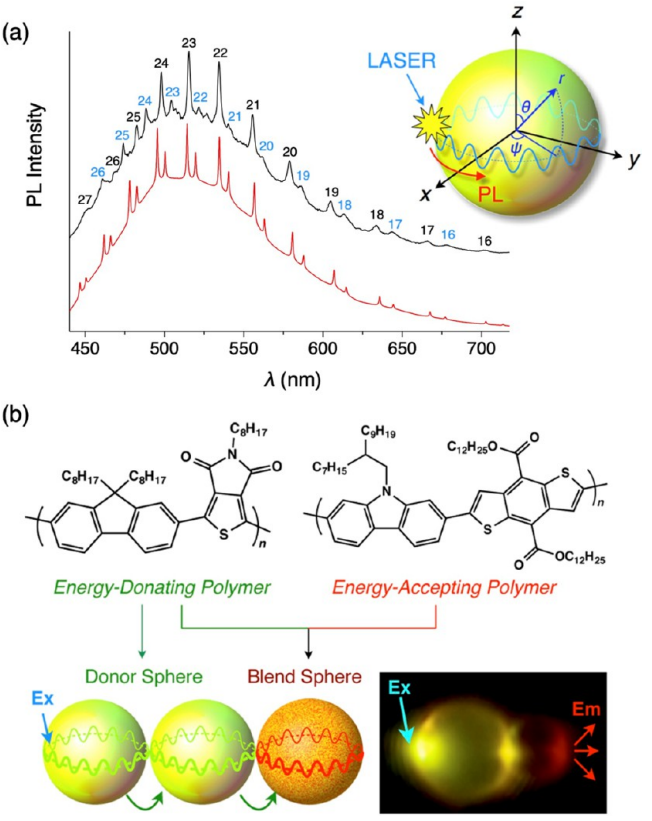

Figure 5. (a) PL spectrum from a single microsphere of F8TMT2 (black curve). The black and blue numbers indicate azimuthal mode numbers (*l*) of the TE and TM mode, respectively. The red curve indicates a simulated spectrum. Inset shows schematic representation of the light confinement and interference via circular propagation at the polymer/air interface. (b) Schematic representation of a polymer blend microsphere composed of energy-donating and -accepting π-conjugated polymers and FM image of intersphere light energy transfer and conversion upon excitation of the energy-donating polymer microsphere. Panel a reproduced from ref 3. Copyright 2014 Springer Nature. Panel b reproduced from ref 19. Copyright 2016 American Chemical Society.

sharp PL lines are attributed to WGMs, where PL generated at the surface of the microsphere is confined circularly via TIR at the polymer/air interface and interferes with itself after traveling around the circumference (Figure 5a, inset). Transverse electric (TE) and magnetic (TM) modes are observed separately, which is characteristic for WGMs in a microsphere resonator.[30] The WGM PL is observed from various microspheres formed from isolated π-conjugated polymers,[22] polycarbazoles,[23] π-conjugated block copolymers,[24] and π-conjugated dendrimers.[25]

https://doi.org/10.1021/acs.accounts.3c00084
Acc. Chem. Res. 2023, 56, 1469−1481

Self-assembled microspheres composed of energy-donating and -accepting polymers display efficient intrasphere energy transfer (Figure 5b).[19] The polymers with appropriate combination, in which two polymers are miscible with one another without phase separation, and molecular weight can form microspheres. In comparison with cast films from solution of these polymers, the polymer blend microspheres display higher energy transfer efficiency due to the light confinement inside the microsphere. Furthermore, by connecting several polymer microspheres, intersphere energy transfer can take place along several microspheres. The intersphere energy transfer was further studied with boron-dipyrrine (BODIPY)-doped polystyrene (PS) microspheres.[26] Depending on the difference of the initial concentration of the doped BODIPY, the PS microspheres display WGM PL with green, yellow, orange, and red colors. The cavity-mediated energy transfer was investigated by coupling two microspheres with different PL colors, where the energy transfer efficiency virtually follows the Förster resonant energy transfer (FRET) law, proportional to the product of PL quantum yield (ϕ_{PL}) and spectral overlap between the absorption band of the acceptor and the emission band of the donor. However, the distance between donor and acceptor reaches several-micrometer scale, which is more than 2 orders of magnitude longer than conventional FRET between molecules (<6 nm). Using the polymer blend system, FRET-mediated near-infrared (NIR) WGM emission is achieved by doping a NIR-emitting conjugated polymer as the energy acceptor in the energy-donating F8TPD microsphere.[20]

We found that continuous, strong excitation of F8TPD microspheres induces WGM splitting.[27] The optically induced mode splitting is caused by photodegradation of conjugated polymers by the photoexcitation, which breaks the spherical symmetry of the microresonator and thus leads to a lifting of the optical degeneracy of the WGM.

3.2. Lasers, Memories, and Logic Gates from π-Conjugated Polymer Microresonators

In order to achieve lasing action from the WGM microresonators, several conditions are required: population inversion to induce stimulated emission and no excited-state absorption of the polymers at the lasing wavelength that would reduce the efficiency of the stimulated emission. To satisfy these requirements, high density optical pumping with a short pulse is necessary, and the polymers have to be robust against the strong pumping. To avoid excited state absorption, we selected poly[9,9-di-*n*-ocylfluorenyl-2,7-diyl] (F8), poly[(9,9-di-*n*-ocylfluorenyl-2,7-diyl-*alt*-benzo[2,1,3]thiadiazol-4,8-diyl) (F8BT), and poly[2-methoxy-5-(3,7-dimethyloctyloxy)-1,4-phenylenevinylene] (MDMOPPV), which are known as laser dyes. Upon femtosecond pumping at 397 nm, these microspheres display lasing actions above the threshold power densities (P_{th}) of 1.5, 58, and 24 μJ cm^{-2} for the microspheres of F8, F8BT, and MDMOPPV, respectively (Figure 6).[31] The P_{th} value was reduced by one-fourth by coating the substrate with a thin Ag layer, so that the mirror effect of the Ag layer enhanced the light confinement efficiency. Energy transfer-assisted lasing was achieved from microspheres with Eu^{3+}-coordinated fluorene-terpyridine alternating copolymer (F8tpy), where red-color lasing emission was observed at 615−630 nm via energy transfer from F8tpy to Eu^{3+}.[32]

The switching operation of WGM PL and lasing is important for applications in optical devices such as optical memory and logic gates. For this purpose, photoswitchable diarylethene

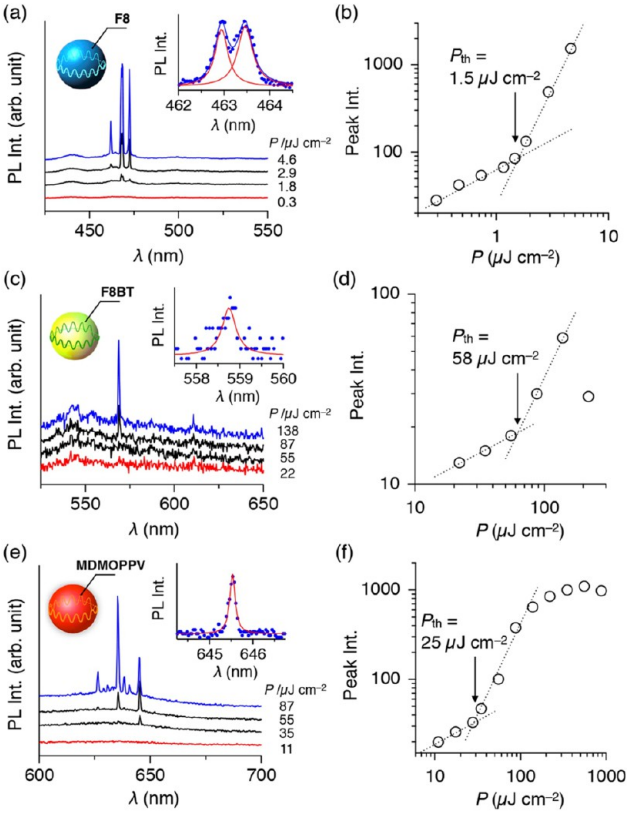

Figure 6. PL spectra (a, c, e) and plots of the intensity of the PL peak versus P (b, d, f) of a single microsphere of F8 (a), F8BT (c), and MDMOPPV (e) on a quartz substrate upon excitation with a fs-laser. Reproduced from ref 31. Copyright 2017 Wiley.

(DAE) is applicable for the WGM switching (Figure 7a, left). By the vapor diffusion method, DAE self-assembles to form well-defined microspheres. Upon photoexcitation at 400−440 nm, the microspheres of closed-form DAE display yellow-colored PL that exhibits clear WGMs. Photoisomerization between fluorescent closed-form and nonfluorescent open-form DAE can switch the WGM PL repeatedly (Figure 7a, right).[4] DAE microspheres are also formed by simply drop casting a solution of DAE in EtOH onto a substrate and allowing the solvent to evaporate. In this case, the spherical shape is not perfect but somewhat distorted. The oblate microspheres exhibit complicated WGM splitting, and the mode splitting is exactly reproduced by finite-difference time-domain (FDTD) simulations (Figure 7b).

The drop-casting and subsequent evaporation method is applicable for fabricating photoswitchable microresonator optical memory arrays. A toluene solution of DAE was drop cast onto a quartz substrate, which was prepatterned with hydrophobic and hydrophilic lines and boxes of 4 μm and 2 μm width, respectively. The cast film of DAE on the prepatterned substrate was immersed into a H_2O/acetone mixed solvent, and surface self-assembly of DAE took place to form a hemispherical microarray. The WGM spectral patterns from all the pixels are different because the shape and size of all pixels are somewhat different from one another (Figure 7c). Accordingly, the optical memory array provides a physically uncloneable function (PUF) and can be utilized as an anti-counterfeiting two-step authentication system; the first step is a micrometer-scale QR code and the second step is reading of the WGM fingerprint from each hemisphere pixel. The surface self-assembly process

https://doi.org/10.1021/acs.accounts.3c00084
Acc. Chem. Res. 2023, 56, 1469−1481

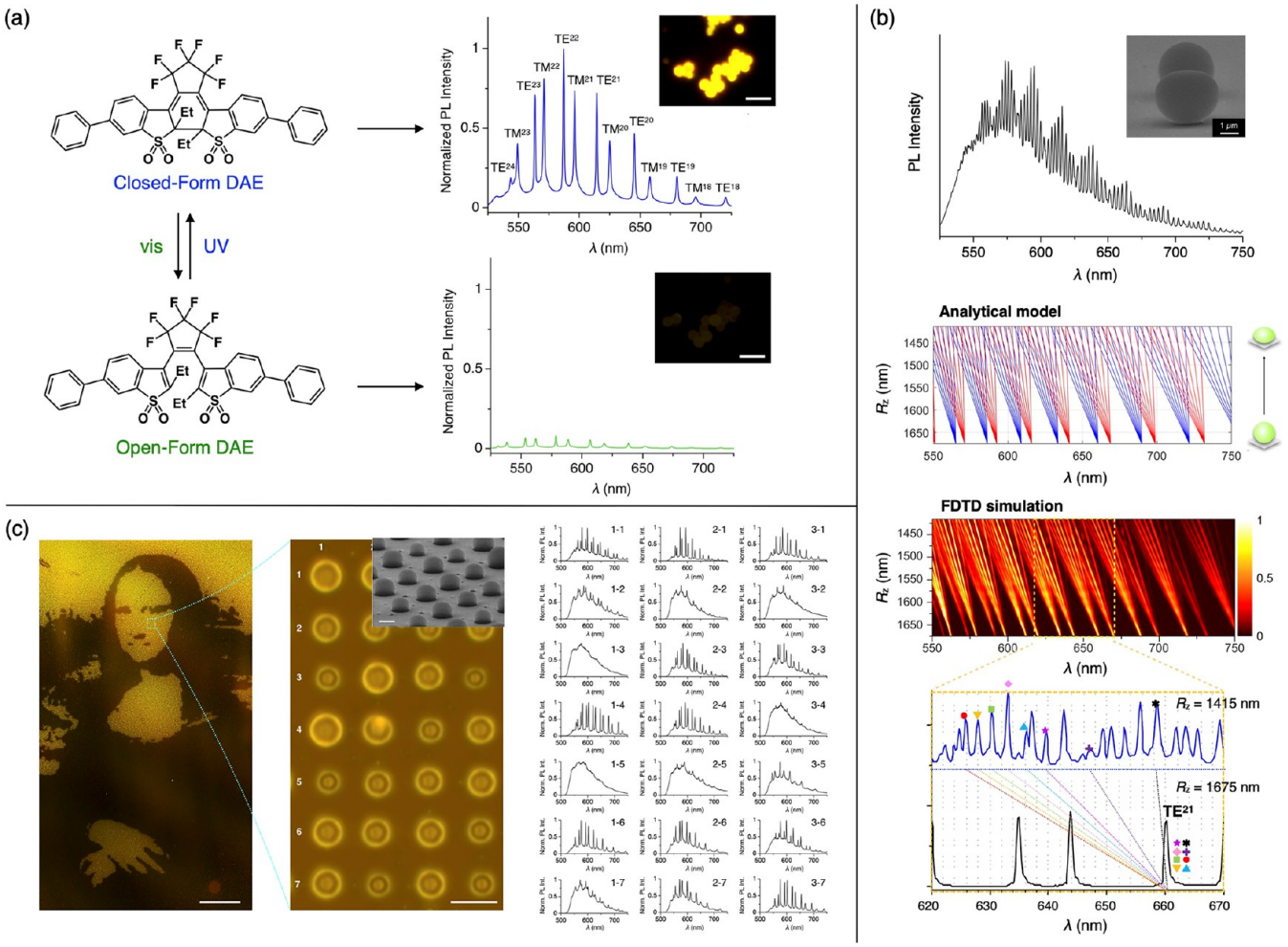

Figure 7. (a, left) Molecular structures of closed-form (top) and open-form (bottom) DAE, which are photoisomerizable with one another upon irradiation to visible and UV light, respectively. (a, right) PL spectra from a single microsphere of closed-form (top) and open-form (bottom) DAE. Insets show FM images of the corresponding microspheres. (b) PL spectrum showing WGM splitting of an oblate DAE microsphere and peak positions with respect to deformation obtained by analytical model and FDTD simulation. (c, left) FM image of a micropainting drawn on a quartz substrate. Scale bar: 300 μm. (c, center) OM image of the microhemisphere array. Scale bar: 5 μm. Inset shows an SEM image of the array. (c, right) PL spectra from each microhemisphere. Scale bar: 2 μm. Reproduced from ref 4. Copyright 2020 Royal Society of Chemistry.

for the fabrication of microdisk arrays is applicable for other organic materials such as PS and π-conjugated polymers.[33]

Photoswitchable microresonators can be utilized in all-organic, all-optical logic gate operations. As described in section 3.1, a cavity-mediated energy transfer cascade occurs efficiently between multiple coupled microspheres.[26] Here, optical gate operation is achieved by making the central microsphere of a triple sphere chain photoswitchable (see Figure 8).[34] When the sphere on the left side is photoexcited, blue emission is generated and transferred to the central DAE-doped microsphere, and in the case where the DAE is in the closed form, further energy transfer cascade occurs to the microsphere on the right side as red WGM PL (output ON). Upon irradiation of the central sphere with visible light, the closed-form DAE is photoisomerized to the open form, resulting in the inhibition of the energy transfer cascade from left to right (output OFF). UV irradiation of the central microsphere changes DAE back to the closed-form, recovering the green-fluorescence of the central sphere and turning on the cascade again (output ON). The cavity-mediated energy transfer cascade is operable when three spheres are directly coupled in series, but the efficiency drops off when the spheres are separated. To achieve energy transfer over much longer distances, we have utilized a PS microfiber as an optical waveguide and placed three spheres separately on the PS fiber (Figure 8a). The optical gate operation is accomplished even when the adjacent microspheres are separated by 2.5 μm. The optical gate is further extended to an OR gate, where two photoswitchable WGM microspheres are set in parallel at the central part (Figure 8b).

Instead of PS microfibers, natural protein fiber made of spider dragline silk can be utilized as an optical fiber, and the same optical logic function can be achieved.[35] The optical loss coefficient of the dragline silk fiber was evaluated as 0.03 dB μm^{-1}, which is smaller by one-fourth in comparison with the PS microfiber (0.13 dB μm^{-1}). An example of optical logic gate operation using dragline silk fibers and photoswitchable microspheres is shown in Figure 8c.

3.3. Optical Sensing Using WGM Microresonators

WGM microresonators can be utilized as highly sensitive optical sensors due to their sharp fluorescent spectral peaks that shift, split, and change their intensity in response to a change in size, morphology, and refractive index of the resonator. Such changes in bulk properties are in contrast to inorganic WGM

https://doi.org/10.1021/acs.accounts.3c00084
Acc. Chem. Res. 2023, 56, 1469−1481

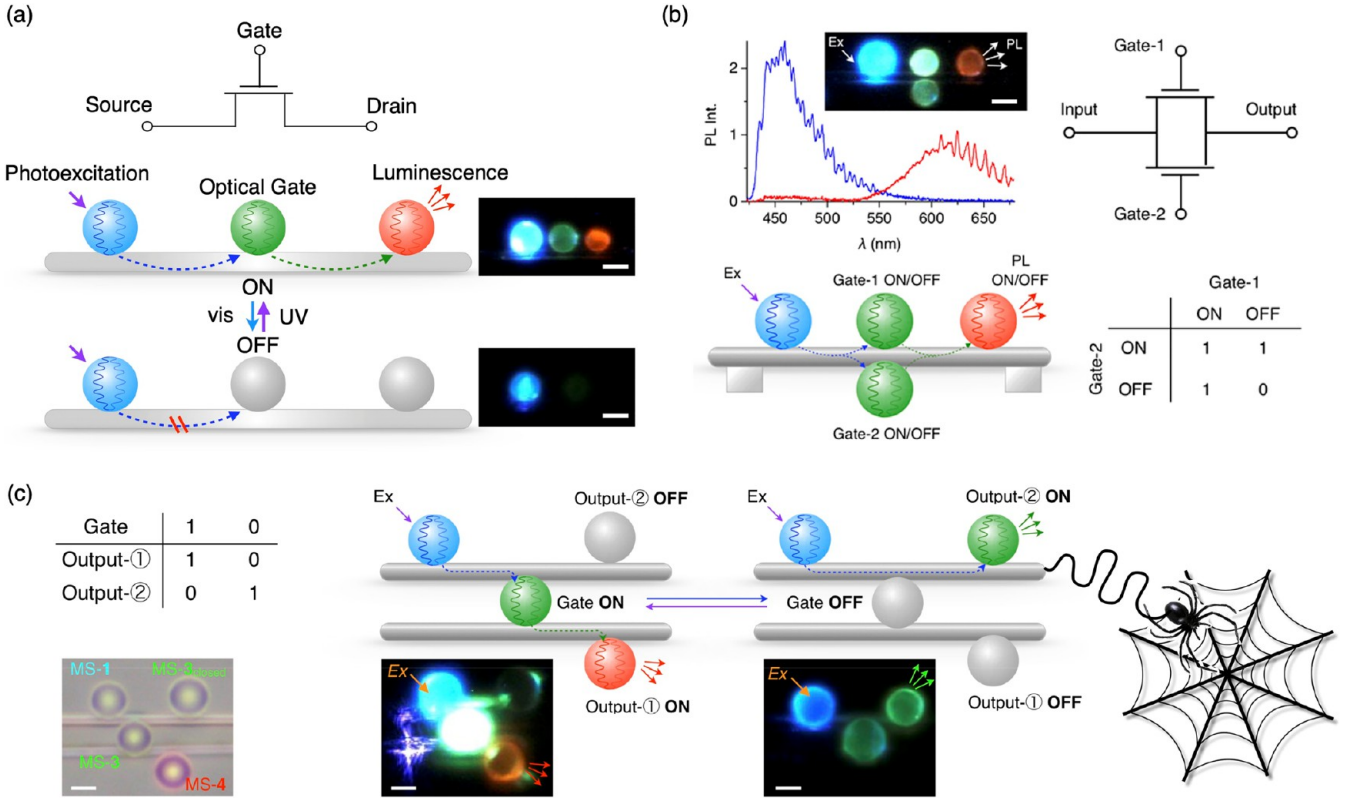

Figure 8. (a) Schematic representations of an electronic gate (top) and an optical gate (bottom). In the optical gate, blue-, green- and red-emitting WGM microspheres are located on an optical fiber. The central microsphere works as an optical gate, which transmits or stops the light transfer cascade. To the right are FM images with gate-on (top) and off (bottom) upon excitation of the left WGM microsphere. (b) Demonstration and schematic representation of four-terminal OR gate and matrices of the optical gate operation with four WGM microspheres on a PS microfiber. (c) Demonstration and schematic representation of a switching gate of the opposite output using four WGM microspheres on two dragline silk microfibers. Scale bars: 3 μm. Panel a reproduced from ref 34. Copyright 2021 Wiley. Panel b Reproduced from ref 35. Copyright 2023 Wiley.

microresonators, where the WGM peak shift occurs only by the refractive index change in response to the adsorption of gases and chemicals on its surface. For example, microspheres consisting of a luminogen-appended hygroscopic polymer work as humidity sensors, where the sensitivity of the WGM peak shift is as high as 0.255 nm for one percent change in relative humidity (%RH), which is the highest among nontapered type optical humidity sensors.[36] Microspheres made from silk fibroin, produced by the mulberry silkworm, which is also hygroscopic, exhibit WGM PL peak shifts of 0.187 nm per %RH at a wide humidity range up to 95%RH.[37]

Polymer microresonators can also be utilized as sensors for volatile organic compounds (VOCs) and acid/base atmospheres. WGM peaks of fluorescent dye-doped PS microspheres shift sensitively in the presence of VOCs, especially aromatic hydrocarbons such as benzene, toluene, and xylene (BTXs).[38] Furthermore, fluorescent microspheres made of a polymer with intrinsic microporosity (PIM-1) display VOC sensing with excellent sensitivity of 0.40 nm ppm^{-1} for pyridine vapor with the limit-of-detection (LOD) as low as 470 ppb without losing its linearity down to 800 ppb (Figure 9a).[39] The high sensitivity and low LOD is attributed to the strong interaction between the electron-rich pyridine and electron-deficient terephthalonitrile moiety in PIM-1. Microspheres from F8tpy are sensitive to acid, where the terpyridine moiety is protonated by immersing the microspheres into a MeOH solution of camphorsulfonic acid, resulting in a large spectral shift (>100 nm).[40] The fluorescence shift recovers when the microspheres are immersed in an alkaline solution.

In addition to the chemical sensing, air-flow sensing is also possible using liquid droplet WGM microresonators (Figure 9b).[41] To avoid evaporation, a nonvolatile ionic liquid is used as a medium, doped with ionic fluorescent dye, and pipetted onto a superhydrophobic substrate to form droplets with sizes and contact angles of 19−4800 μm and 140−166°, respectively. The resultant microdroplets display WGM lasing upon nanosecond-laser excitation with P_{th} of 1.21 μJ cm^{-2}, which is only one twentieth of that of a poly(vinyl alcohol) (PVA) microsphere (23.4 μJ cm^{-2}). Because of the liquid nature, the droplet resonator deforms under gas convection, leading to a spectral shift of the lasing peak. The LOD of the flow rate is as low as 0.13 m s^{-1}, which is comparable to the other existing microscopic flowmetric techniques. Furthermore, the ionic liquid droplet array can be fabricated using an inkjet printer, where the size and position of the droplets is finely controlled.

Degradation reactions of insoluble polymers are of fundamental importance in a variety of industrial processes such as fermentation, digestion, and environmental decomposition. Therefore, monitoring their reaction kinetics has been a formidable challenge. In our recent study,[42] the WGM spectrum of an insoluble silk fibroin microsphere was observed in water that contains enzymes,[37] and the reaction kinetics was successfully monitored as spectral changes with high precision and fast response time. When using proteinase K that is capable of hydrolyzing fibroin proteins of silk, the resonance peaks

https://doi.org/10.1021/acs.accounts.3c00084
Acc. Chem. Res. 2023, 56, 1469−1481

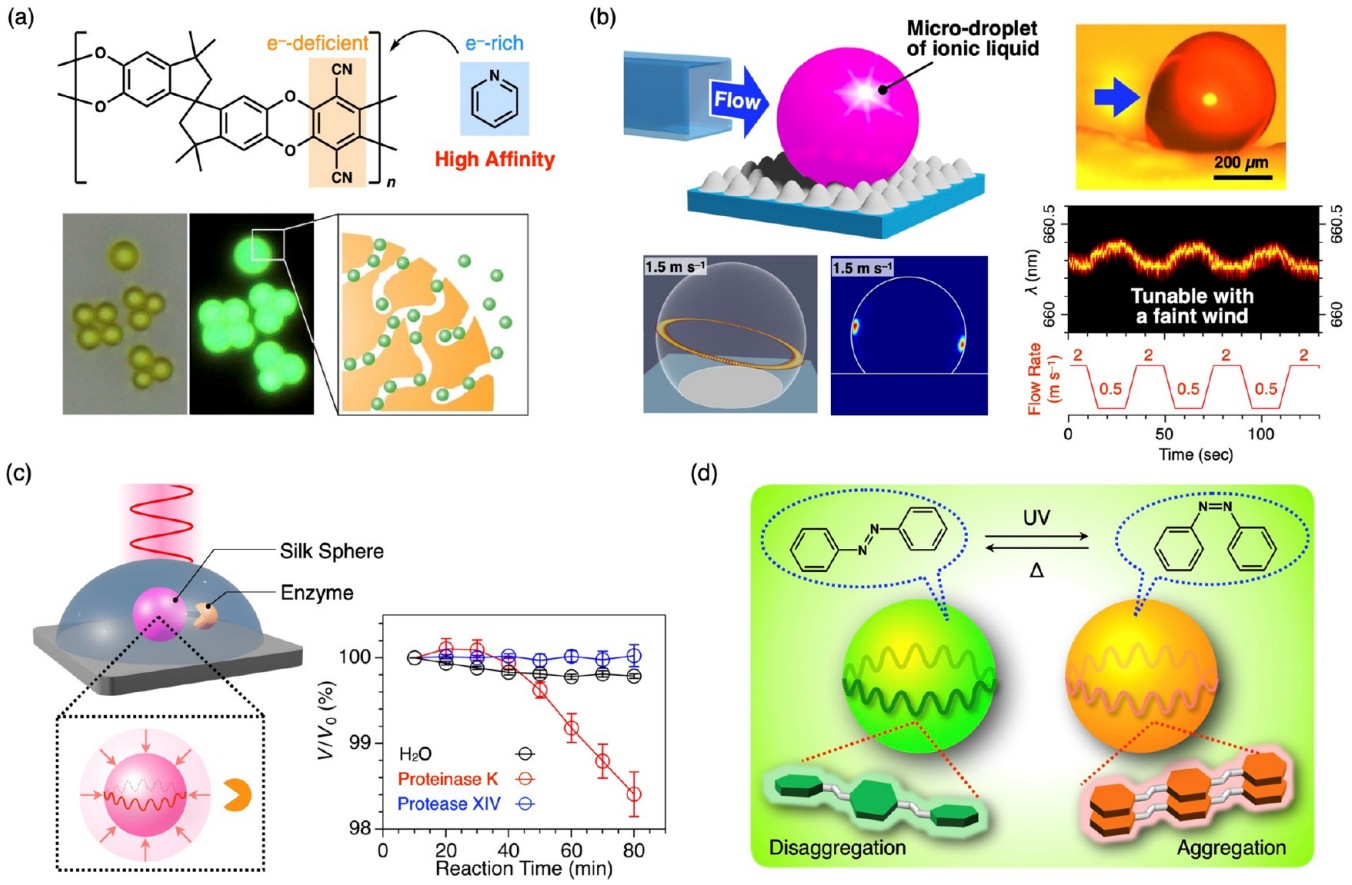

Figure 9. (a) Molecular structure of PIM-1 and schematic representation of the porous microsphere that works as a highly sensitive VOC sensor. (b) Schematic representation of microdroplet made of ionic liquid that works as a micro-flow sensor. (c) WGM optical monitoring of deterioration of a silk microsphere by enzymatic reaction. (d) Schematic representation of optical control of aggregation/disaggregation in a liquid droplet by photoisomerization of azobenzene. Panel a reproduced from ref 39. Copyright 2022 American Chemical Society. Panel b reproduced from ref 41. Copyright 2023 Wiley. Panel c reproduced from ref 42. Copyright 2023 Royal Society of Chemistry. Panel d Reproduced from ref 43. Copyright 2023 Wiley.

gradually and monotonically blue-shifted with time. This change in peak position was attributed to the enzymatic degradation of the silk proteins and the associated decrease in diameter of the sphere (Figure 9c).

Optical control of the resonance peaks is of practical importance for future all-optical logic devices. As shown in section 3.2, the chemical strategy is the incorporation of photochromic dyes into the resonator matrix that alter their luminescence color and intensity upon isomerization reaction.[35,36] We also succeeded in the same goal by using a different chemistry. A droplet WGM resonator was synthesized, which incorporated a luminescent dye together with a nonluminescent photoisomer. The photoisomerization of the isomer drastically changed the solubility of the luminescent dye in the liquid matrix and thereby changed the luminescent color and intensity of the droplet resonator. This strategy is made possible by the photoisomer, which is a special type of azobenzene derivative. The *trans*-form isomer is insoluble to the droplet and thereby increases the solubility of the luminescent dye in the liquid, while the *cis*-form isomer is soluble to the droplet and thereby precipitates out the dye from the liquid. This strategy is unique in that the luminescent dyes themselves do not have to be photoisomerizable (Figure 9d).[43]

3.4. Precise Synthesis of Microcrystals from π-Conjugated Molecules for Microlasers

Microcrystals work as optical resonators, where the crystalline facets act as TIR mirrors and confine light inside the crystal. Carbon-bridged oligo(*para*-phenylene vinylene)s (COPVs) are excellent laser dyes with high ϕ_{PL} and stability against optical pumping due to their rigid π-conjugated plane isolated with the aryl side chains (Figure 10a).[44] The microcrystals are fabricated by surface crystallization: Solutions of COPV2 and COPV3 are drop-cast onto a quartz substrate, and the solvent is slowly evaporated.[45] The resultant rhombic platelet microcrystals of COPV2 and COPV3, lying on the substrate, display WGM lasing upon fs-pumping with P_{th} of 35 and 18 μJ cm^{-2}, respectively (Figure 10b). Solutions of COPV2/COPV3 mixture also yielded rhombic crystals, which show WGM lasing upon strong fs pumping above P_{th}. Interestingly, upon weak excitation below P_{th}, energy transfer occurs efficiently from COPV2 to COPV3 in the cocrystals, resulting in green-colored luminescence. In contrast, upon strong excitation, the lasing from the cocrystals occurs only by the luminescence from COPV2 without energy transfer. The time-resolved PL decay studies indicate that the lasing occurs with a rate constant (k_{lasing}) of 4.0×10^{10} s^{-1}, which is 20 times faster than that of FRET (k_{FRET}, 1.8×10^{9} s^{-1}). Noteworthy, P_{th} can be reduced by one-fourth by using a 50 nm thick Ag-coated quartz substrate,

https://doi.org/10.1021/acs.accounts.3c00084
Acc. Chem. Res. 2023, 56, 1469−1481

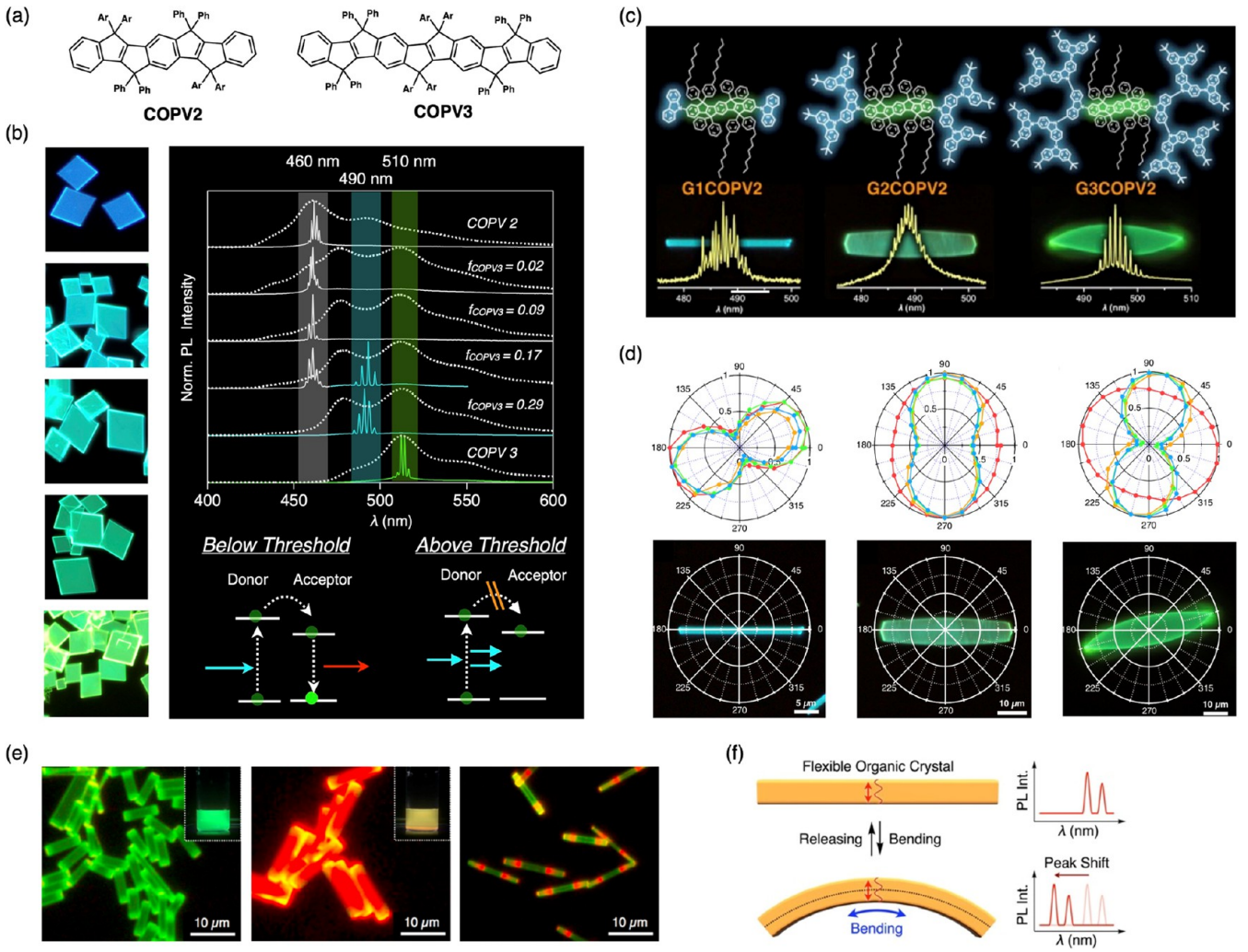

Figure 10. (a) Molecular structures of COPV2 and COPV3. (b) FM images of microcrystals with f_{COPV3} = 0, 0.019, 0.063, 0.130, and 1 (left, from top to bottom), PL spectra from the microcrystals (right), and schematic representations of the energy transfer and lasing below and above P_{th} (right, bottom). (c) Molecular structures of G1-, G2-, and G3COPV2, and PL spectra from a single microcrystal upon fs-pumping. (d) Plots of polarization-dependent normalized gray values of the luminescence intensity for microcrystals of G1-, G2-, and G3COPV2. (e) FM images of green (left), red (center), and optically heterostructured BODIPY microrods. Insets show the appearance of the microcrystals in solution under UV illumination. (f) Schematic representation of FOC with FP resonator properties. Panel a reproduced from ref 45. Copyright 2018 American Chemical Society. Panel b Reproduced from ref 46. Copyright 2020 Wiley. Panel c reproduced from ref 47. Copyright 2019 American Chemical Society. Panel d reproduced from ref 48. Copyright 2022 Wiley.

where the resultant platelet microcrystals grow vertically. The small contact area with the substrate, as well as the mirror effect of the Ag layer, reduces P_{th} remarkably.

Crystallization of COPV2 bearing light-harvesting first-, second-, and third-generation carbazole dendrons (G*n*COPV2, n = 1, 2, 3, respectively) was investigated.[46] Under appropriate vapor diffusion conditions, G*n*COPV2 forms microcrystals with rod (n = 1), platelet (n = 2), and leaf-like (n = 3) morphologies (Figure 10c). Because the carbazole groups in the microcrystal of G3COPV2 have almost omnidirectional orientation, the G3-dendrons harvest light in any polarized direction and transfer its energy to the COPV2 core (Figure 10d). The microcrystals display lasing upon fs-pumping. FDTD simulations indicate that the rod-shaped G1COPV2 microcrystal works as a FP-mode resonator, while G2COPV2 and G3COPV2 microcrystals confine light with a bow-tie mode and WGM, respectively. The P_{th} value is the lowest for the G2COPV2 microcrystal (~66 μJ cm^{-2}) for the following two reasons: (1) the high light confinement efficiency due to the small light leakage at the crystalline edge and (2) preferable molecular orientation of the COPV2 core that coincides with the direction of the light confinement.

Another interesting type of microcrystal is formed from BODIPY, where the green- and red-colored luminescent domains appear alternately in a single microrod crystal (Figure 10e).[47] The red-colored domains involve defect sites with a small band gap, which is confirmed by temperature-dependent PL spectral change and time-resolved microwave conductivity studies. Flexible organic microcrystals (FOCs) work as FP resonators, which can monitor the mechanical distortion of the crystals (Figure 10f).[48] The resonant peaks shift upon mechanical bending, and the shifts are repeated for more than 50 cycles without deterioration in their mechanical and optical properties.

4. CONCLUSIONS AND OUTLOOK

In summary, we have developed precise design and control of organic/polymeric microstructures by bottom-up self-assembly

https://doi.org/10.1021/acs.accounts.3c00084
Acc. Chem. Res. 2023, 56, 1469−1481

processes in solution and on a substrate surface. The morphologies of the microstructures are spheres, hemispheres, rods, plates, and concave hexagonal pyramids, in which the shapes, molecular orientation and arrangement are controlled by the hierarchical control of the growth conditions. The resultant microstructures display characteristic optical functionality such as WGM resonators and lasers, CPL emitters, light-harvesters, and energy converters and can furthermore be utilized as optical memories, logic gates, and optical sensors for humidity, VOCs, airflow, and mechanical distortion. The developed strategies for fabricating microstructures with sophisticated designs and functions will be valuable for future research on organic electronics and photonics in both fundamentals and applications.

A practical benefit of the bottom-up approach is the scalability. The organic microstructures introduced herein can be produced by a simple solution technique. This feature is beneficial for producing metasurfaces, displays, and sensors. The susceptibility of organic molecules to chemical, physical, and biological stimuli is also valuable. As demonstrated by our work, optical resonators and lasers can function as precise sensors. This feature can be enhanced by using tailored organic molecules as the host of the resonators. Likewise, the chemical and biological selectivity can be enhanced by designing the host molecule as such.

AUTHOR INFORMATION

Corresponding Author

Yohei Yamamoto − *Department of Materials Science, Faculty of Pure and Applied Sciences, and Tsukuba Research Center for Energy Materials Science (TREMS), University of Tsukuba, Tsukuba, Ibaraki 305-8573, Japan;* orcid.org/0000-0002-2166-3730; Email: yamamoto@ims.tsukuba.ac.jp

Authors

Hiroshi Yamagishi − *Department of Materials Science, Faculty of Pure and Applied Sciences, and Tsukuba Research Center for Energy Materials Science (TREMS), University of Tsukuba, Tsukuba, Ibaraki 305-8573, Japan;* orcid.org/0000-0003-3184-4217

Jer-Shing Huang − *Leibniz Institute of Photonic Technology, 07745 Jena, Germany; Institute of Physical Chemistry and Abbe Center of Photonics, Friedrich-Schiller-Universität Jena, D-07743 Jena, Germany; Research Center for Applied Sciences, Academia Sinica, Taipei 11529, Taiwan; Department of Electrophysics, National Yang Ming Chiao Tung University, Hsinchu 30010, Taiwan;* orcid.org/0000-0002-7027-3042

Axel Lorke − *Faculty of Physics and Center for Nanointegration Duisburg-Essen (CENIDE), University of Duisburg-Essen, Duisburg D-47048, Germany;* orcid.org/0000-0002-0405-7720

Complete contact information is available at: https://pubs.acs.org/10.1021/acs.accounts.3c00084

Author Contributions

CRediT: **Yohei Yamamoto** conceptualization (lead), resources (lead), visualization (lead), writing-original draft (lead), writing-review & editing (lead); **Hiroshi Yamagishi** conceptualization (supporting), resources (supporting), visualization (supporting), writing-original draft (supporting), writing-review & editing (supporting); **Jer-Shing Huang** conceptualization (supporting), formal analysis (supporting), investigation (supporting), methodology (supporting), writing-review & editing (supporting); **Axel Lorke** conceptualization (supporting), writing-review & editing (supporting).

Notes

The authors declare no competing financial interest.

Biographies

Yohei Yamamoto received his doctoral degree in 2003 from Osaka University under supervision of Prof. Tomoji Kawai. From 2004, he joined Aida Nanospace Project, JST, as a postdoctoral researcher. In 2010, he was appointed as an associate professor in University of Tsukuba, and in 2018, he was promoted to a full professor in the same university. His research interests are molecular self-assembly and the photonic and laser properties of the resulting materials.

Hiroshi Yamagishi received his doctoral degree in Engineering in 2018 from The University of Tokyo under supervision of Prof. Takuzo Aida. After graduation, he joined the research group of Prof. Yamamoto in University of Tsukuba as an assistant professor. His research focuses on supramolecular chemistry and crystal engineering in conjunction with the optical and laser properties of the resulting materials.

Jer-Shing Huang received his doctoral degree in Chemistry in 2004 from National Taiwan University. He continued with his research as a postdoctoral research fellow at the Academia Sinica (2004−2006, on single-molecule microscopy) in Taiwan and University of Würzburg (2007−2010, on plasmonic nanoantennas) with Prof. Bert Hecht in Germany. In 2010, he was appointed as an assistant professor at National Tsing Hua University, and in 2015, he was promoted to associate professor at the same university. In 2016, he moved to the Leibniz Institute of Photonic Technology in Germany, leading the Research Department of Nanooptics. His research interests include nanoplasmonics, chiral light−matter interaction, and optical microresonators.

Axel Lorke is professor of experimental physics at the University of Duisburg-Essen. He received his Ph.D. from the Ludwig Maximilian University (LMU) of Munich and held postdoctoral positions at University of Tokyo, University of California, Santa Barbara, and LMU Munich. His research interests are low-dimensional semiconductors and their quantum properties, optical and transport spectroscopy of novel materials, and functional micro- and nanostructures.

ACKNOWLEDGMENTS

This work was supported by CREST (JPMJCR20T4) and ACT-X (JPMJAX201J) from Japan Science and Technology Agency (JST), Grant-in-Aid for Scientific Research on Innovative Areas (JP17H05142), Scientific Research (A) (JP16H02081), and Young Scientist (JP19J20398) from Japan Society for the Promotion of Science (JSPS), bilateral joint research program between JSPS and DAAD (BBD30033 and 57402047).

REFERENCES

(1) Oki, O.; Kulkarni, C.; Yamagishi, H.; Meskers, S. C. J.; Lin, Z.-H.; Huang, J.-S.; Meijer, E. W.; Yamamoto, Y. Robust Angular Anisotropy of Circularly Polarized Luminescence from a Single Twisted-bipolar Polymeric Microsphere. *J. Am. Chem. Soc.* **2021**, *143*, 8772−8779.

(2) Oki, O.; Yamagishi, H.; Morisaki, Y.; Inoue, R.; Ogawa, K.; Miki, N.; Norikane, Y.; Sato, H.; Yamamoto, Y. Synchronous assembly of chiral skeletal single-crystalline microvessels. *Science* **2022**, *377*, 673−678.

(3) Tabata, K.; Braam, D.; Kushida, S.; Tong, L.; Kuwabara, J.; Kanbara, T.; Beckel, A.; Lorke, A.; Yamamoto, Y. Self-Assembled

Conjugated Polymer Spheres as Fluorescent Microresonators. *Sci. Rep.* **2014**, *4*, 5902.
(4) Okada, D.; Lin, Z.-H.; Huang, J.-S.; Oki, O.; Morimoto, M.; Liu, X.; Minari, T.; Ishii, S.; Nagao, T.; Irie, M.; Yamamoto, Y. Optical microresonator arrays of fluorescence-switchable diarylethenes with unreplicable spectral fingerprints. *Mater. Horiz.* **2020**, *7*, 1801−1808.
(5) Samuel, I. D. W.; Turnbull, G. A. Organic Semiconductor Lasers. *Chem. Rev.* **2007**, *107*, 1272−1295.
(6) Zhang, Q.; Tao, W.; Huang, J.; Xia, R.; Cabanillas-Gonzalez, J. Toward Electrically Pumped Organic Lasers: A Review and Outlook on Material Developments and Resonator Architectures. *Adv. Photon. Res.* **2021**, *2*, 2000155.
(7) Zhang, W.; Yao, J.; Zhao, Y. S. Organic Micro/Nanoscale Lasers. *Acc. Chem. Res.* **2016**, *49*, 1691−1700.
(8) Wei, G.-Q.; Wang, X.-D.; Liao, L.-S. Recent Advances in 1D Organic Solid-State Lasers. *Adv. Funct. Mater.* **2019**, *29*, 1902981.
(9) Wei, G.-Q.; Wang, X.-D.; Liao, L.-S. Recent Advances in Organic Whispering-Gallery Mode Lasers. *Laser Photon. Rev.* **2020**, *14*, 2000257.
(10) Aida, T.; Stupp, S. I.; Meijer, E. W. Functional Supramolecular Polymers. *Science* **2012**, *335*, 813−817.
(11) Yamamoto, Y. Programmed self-assembly of large π-conjugated molecules into electroactive one-dimensional nanostructures. *Sci. Technol. Adv. Mater.* **2012**, *13*, No. 033001.
(12) Beaujuge, P. M.; Fréchet, J. M. J. Molecular Design and Ordering Effects in π-Functional Materials for Transistor and Solar Cell Applications. *J. Am. Chem. Soc.* **2011**, *133*, 20009−20029.
(13) Gierschner, J.; Shi, J.; Milián-Medina, B.; Roca-Sanjuán, D.; Varghese, S.; Park, S.-Y. Luminescence in Crystalline Organic Materials: From Molecules to Molecular Solids. *Adv. Opt. Mater.* **2021**, *9*, 2002251.
(14) Adachi, T.; Tong, L.; Kuwabara, J.; Kanbara, T.; Saeki, A.; Seki, S.; Yamamoto, Y. Spherical assemblies from π-conjugated alternating copolymers: Toward optoelectronic colloidal crystals. *J. Am. Chem. Soc.* **2013**, *135*, 870−876.
(15) Tong, L.; Kushida, S.; Kuwabara, J.; Kanbara, T.; Ishii, N.; Saeki, A.; Seki, S.; Furumi, S.; Yamamoto, Y. Tetramethylbithiophene in π-Conjugated Alternating Copolymers as an Effective Structural Component for the Formation of Spherical Assemblies. *Polym. Chem.* **2014**, *5*, 3583−3587.
(16) Yamamoto, Y. Spherical resonators from π-conjugated polymers. *Polym. J.* **2016**, *48*, 1045−1050.
(17) Jindal, A.; Kotani, H.; Kushida, S.; Saeki, A.; Kojima, T.; Yamamoto, Y. Significant Enhancement of Hole Transport Ability in Conjugated Polymer/Fullerene Bulk Heterojunction Microspheres. *ACS Appl. Polym. Mater.* **2019**, *1*, 118−123.
(18) Kushida, S.; Oki, O.; Saito, H.; Kuwabara, J.; Kanbara, T.; Tashiro, M.; Katouda, M.; Imamura, Y.; Yamamoto, Y. From linear to foldamer and assembly: Hierarchical transformation of a coplanar conjugated polymer into a microsphere. *J. Phys. Chem. Lett.* **2017**, *8*, 4580−4586.
(19) Kushida, S.; Braam, D.; Dao, T. D.; Saito, H.; Shibasaki, K.; Ishii, S.; Nagao, T.; Saeki, A.; Kuwabara, J.; Kanbara, T.; Kijima, M.; Lorke, A.; Yamamoto, Y. Conjugated Polymer Blend Microspheres for Efficient, Long-Range Light Energy Transfer. *ACS Nano* **2016**, *10*, 5543−5549.
(20) Oki, O.; Kushida, S.; Mikosch, A.; Hatanaka, K.; Takeda, Y.; Minakata, S.; Kuwabara, J.; Kanbara, T.; Dao, T. D.; Ishii, S.; Nagao, T.; Kuehne, A. J. C.; Deschler, F.; Friend, R. H.; Yamamoto, Y. FRET-mediated near infrared whispering gallery modes: studies on the relevance of intracavity energy transfer with Q-factors. *Mater. Chem. Front.* **2018**, *2*, 270−274.
(21) Ihara, Y.; Yamagishi, H.; Lin, C.; Jhu, C.-H.; Tsai, M.-C.; Horie, M.; Yamamoto, Y. Hydrothermal crosslinking of poly(fluorenylamine) with styryl side chains to produce insoluble fluorescent microparticles. *Polym. J.* **2023**, *55*, 547−553.
(22) Kushida, S.; Braam, D.; Pan, C.; Dao, T. D.; Tabata, K.; Sugiyasu, K.; Takeuchi, M.; Ishii, S.; Nagao, T.; Lorke, A.; Yamamoto, Y. Whispering Gallery Resonance from Self-Assembled Microspheres of Highly Fluorescent Isolated Conjugated Polymers. *Macromolecules.* **2015**, *48*, 3928−3933.
(23) Kushida, S.; Okabe, S.; Dao, T. D.; Ishii, S.; Nagao, T.; Saeki, A.; Kijima, M.; Yamamoto, Y. Self-assembled polycarbazole microspheres as single-component, white colour resonant photoemitters. *RSC Adv.* **2016**, *6*, 52854−52857.
(24) Lin, Y.-J.; Chiang, H.-Y.; Oki, O.; Kushida, S.; Chiu, S.-T.; Chang, S.-W.; Yamamoto, Y.; Hosokai, T.; Horie, M. Conjugated copolymers of poly(arylenevinylene)s: synthesis by ring-opening metathesis polymerization, film morphology, and resonant luminescence from microspheres. *ACS Appl. Polym. Mater.* **2019**, *1*, 2240−2248.
(25) Albrecht, K.; Minagawa, K.; Nakajima, S.; Kushida, S.; Yamamoto, Y.; Kuzume, A.; Yamamoto, K. Nanosphere Formation of π-Conjugated Dendrimers by Simple Precipitation Method. *Chem. Lett.* **2019**, *48*, 1240−1243.
(26) Okada, D.; Nakamura, T.; Braam, D.; Dao, T. D.; Ishii, S.; Nagao, T.; Lorke, A.; Nabeshima, T.; Yamamoto, Y. Color-Tunable Resonant Photoluminescence and Cavity-Mediated Multistep Energy Transfer Cascade. *ACS Nano* **2016**, *10*, 7058−7063.
(27) Braam, D.; Kushida, S.; Niemöller, R.; Prinz, G. M.; Saito, H.; Kanbara, T.; Kuwabara, J.; Yamamoto, Y.; Lorke, A. Optically induced mode splitting in self-assembled, high quality-factor conjugated polymer microcavities. *Sci. Rep.* **2016**, *6*, 19635.
(28) Di Nuzzo, D.; Kulkarni, C.; Zhao, B.; Smolinsky, E.; Tassinari, F.; Meskers, S. C. J.; Naaman, R.; Meijer, E. W.; Friend, R. H. High circular polarization of electroluminescence achieved via self-assembly of a light-emitting chiral conjugated polymer into multidomain cholesteric films. *ACS Nano* **2017**, *11*, 12713−12722.
(29) Gon, M.; Morisaki, Y.; Sawada, R.; Chujo, Y. Synthesis of optically active, X-shaped, conjugated compounds and dendrimers based on planar chiral [2.2]paracyclophane, leading to highly emissive circularly polarized luminescence. *Chem.—Eur. J.* **2016**, *22*, 2291−2298.
(30) Oraevsky, A. N. Whispering-gallery waves. *Quant. Elect.* **2002**, *32*, 377−400.
(31) Kushida, S.; Okada, D.; Sasaki, F.; Lin, Z.-H.; Huang, J.-S.; Yamamoto, Y. Low-Threshold Whispering Gallery Mode Lasing from Self-Assembled Microspheres of Single-Sort Conjugated Polymers. *Adv. Opt. Mater.* **2017**, *5*, 1700123.
(32) Ngara, Z. S.; Okada, D.; Oki, O.; Yamamoto, Y. Energy Transfer-Assisted Whispering Gallery Mode Lasing in Conjugated Polymer/Europium Hybrid Microsphere Resonators. *Chem.—Asian J.* **2019**, *14*, 1637−1641.
(33) Yamagishi, H.; Matsui, T.; Kitayama, Y.; Aikyo, Y.; Tong, L.; Kuwabara, J.; Kanbara, T.; Morimoto, M.; Irie, M.; Yamamoto, Y. Fluorescence switchable conjugated polymer microdisk arrays by cosolvent vapor annealing. *Polymers* **2021**, *13*, 269.
(34) Hendra; Takeuchi, A.; Yamagishi, H.; Oki, O.; Morimoto, M.; Irie, M.; Yamamoto, Y. Photochemically Switchable Interconnected Microcavities for All-Organic Optical Logic Gate. *Adv. Funct. Mater.* **2021**, *31*, 2103685.
(35) Hendra; Yamagishi, H.; Heah, W. Y.; Malay, A. D.; Numata, K.; Yamamoto, Y. Micrometer-Scale Optical Web Made of Spider Dragline Fibers with Optical Gate Operations. *Adv. Opt. Mater.* **2022**, 2202563.
(36) Qiagedeer, A.; Yamagishi, H.; Sakamoto, M.; Hasebe, H.; Ishiwari, F.; Fukushima, T.; Yamamoto, Y. A highly sensitive humidity sensor based on aggregation-induced emission luminogen-appended hygroscopic polymer microresonator. *Mater. Chem. Front.* **2021**, *5*, 799−803.
(37) Heah, W. Y.; Yamagishi, H.; Fujita, K.; Sumitani, M.; Mikami, Y.; Yoshioka, H.; Oki, Y.; Yamamoto, Y. Silk fibroin microspheres as optical resonators for wide-range humidity sensing and biodegradable lasers. *Mater. Chem. Front.* **2021**, *5*, 5653−5657.
(38) Qiagedeer, A.; Yamagishi, H.; Hayashi, S.; Yamamoto, Y. Polymer Optical Microcavity Sensor for Volatile Organic Compounds with Distinct Selectivity toward Aromatic Hydrocarbons. *ACS Omega* **2021**, *6*, 21066−21070.
(39) Tanji, N.; Yamagishi, H.; Fujita, K.; Yamamoto, Y. Nanoporous Fluorescent Microresonators for Non-wired Sensing of Volatile

https://doi.org/10.1021/acs.accounts.3c00084
Acc. Chem. Res. 2023, 56, 1469−1481

Organic Compounds down to the ppb Level. *ACS Appl. Polym. Mater.* **2022**, *4*, 1065−1070.
(40) Ngara, Z. S.; Yamamoto, Y. Modulation of Whispering Gallery Modes from Fluorescent Copolymer Microsphere Resonators by Protonation/Deprotonation. *Chem. Lett.* **2019**, *48*, 607−610.
(41) Yamagishi, H.; Fujita, K.; Miyagawa, J.; Mikami, Y.; Yoshioka, H.; Oki, Y.; Takada, N.; Baba, S.; Saito, S.; Someya, S.; Lin, Z.-H.; Huang, J.-S.; Yamamoto, Y. Pneumatically Tunable Droplet Microlaser. *Laser Photon. Rev.* **2023**, 2200874.
(42) Takeuchi, A.; Heah, W. Y.; Yamamoto, Y.; Yamagishi, H. Degradable Optical Resonator as in situ Micro-probes for Microscopy-based Observation of Enzymatic Hydrolysis. *Chem. Commun.* **2023**, *59*, 1477−1480.
(43) Zhao, S.; Yamagishi, H.; Norikane, Y.; Hayashi, S.; Yamamoto, Y. Optical Control of Aggregation Induced Emission Shift by Photo-isomerizable Precipitant in a Liquid Droplet Microresonator. *Adv. Opt. Mater.* **2023**, *11*, 2202134.
(44) Morales-Vidal, M.; Boj, P. G.; Villalvilla, J. M.; Quintana, J. A.; Yan, Q.; Lin, N.-T.; Zhu, X.; Ruangsupapichat, N.; Casado, J.; Tsuji, H.; Nakamura, E.; Díaz-García, M. A. *Nat. Commun.* **2015**, *6*, 8458.
(45) Okada, D.; Azzini, S.; Nishioka, H.; Ichimura, A.; Tsuji, H.; Nakamura, E.; Sasaki, F.; Genet, C.; Ebbesen, T. W.; Yamamoto, Y. π-Electronic Co-crystal Microcavities with Selective Vibronic-Mode Light Amplification: Toward Förster Resonance Energy Transfer Lasing. *Nano Lett.* **2018**, *18*, 4396−4402.
(46) Iwai, K.; Yamagishi, H.; Herzberger, C.; Sato, Y.; Tsuji, H.; Albrecht, K.; Yamamoto, K.; Sasaki, F.; Sato, H.; Asaithambi, A.; Lorke, A.; Yamamoto, Y. Single-Crystalline Optical Microcavities from Luminescent Dendrimers. *Angew. Chem., Int. Ed.* **2020**, *59*, 12674−12679.
(47) Asaithambi, A.; Okada, D.; Prinz, G.; Sato, H.; Saeki, A.; Nakamura, T.; Nabeshima, T.; Yamamoto, Y.; Lorke, A. Polychromatic Photoluminescence of Polymorph Boron Dipyrromethene Crystals and Heterostructures. *J. Phys. Chem. C* **2019**, *123*, 5061−5066.
(48) Zhao, S.; Yamagishi, H.; Oki, O.; Ihara, Y.; Ichiji, N.; Kubo, A.; Hayashi, S.; Yamamoto, Y. Mechanically Flexible and Optically Tunable Organic Crystal Resonator. *Adv. Opt. Mater.* **2022**, *10*, 2101808.

https://doi.org/10.1021/acs.accounts.3c00084
Acc. Chem. Res. 2023, 56, 1469−1481